AAPS PharmSciTech (2024) 25:28
https://doi.org/10.1208/s12249-024-02738-5

RESEARCH ARTICLE

Rapidly Dissolving Trans-scleral Microneedles for Intraocular Delivery of Cyclosporine A

Hamad Alrbyawi[1,2] · Manjusha Annaji[1] · Oladiran Fasina[3] · Srinath Palakurthi[4] · Sai H. S. Boddu[5,6] · Nageeb Hassan[6,7] · Amit K. Tiwari[8] · Amol Suryawanshi[9] · R. Jayachandra Babu[1]

Received: 9 October 2023 / Accepted: 27 December 2023 / Published online: 1 February 2024

Abstract

Cyclosporine A (CsA) is a cyclic peptide immunosuppressant drug that is beneficial in the treatment of various ocular diseases. However, its ocular bioavailability in the posterior eye is limited due to its poor aqueous solubility. Conventional CsA formulations such as a solution or emulsion permeate poorly across the eye due to various static and dynamic barriers of the eye. Dissolvable microneedle (MN)-based patches can be used to overcome barrier properties and, thus, enhance the ocular bioavailability of CsA in the posterior eye. CsA-loaded dissolvable MN patches were fabricated using polyvinylpyrrolidone (PVP) and characterized for MN uniformity and sharpness using SEM. Further characterization for its failure force, penetration force, and depth of penetration were analyzed using a texture analyzer. Finally, the dissolution time, ex vivo permeation, and ocular distribution of cyclosporine were determined in isolated porcine eyes. PVP MNs were sharp, uniform with good mechanical properties, and dissolved within 5 min. Ocular distribution of CsA in a whole porcine eye perfusion model showed a significant increase of CsA levels in various posterior segment ocular tissues as compared to a topically applied ophthalmic emulsion (Restasis®) ($P < 0.001$). Dissolving MNs of CsA were prepared, and the MN arrays can deliver CsA to the back of the eye offering potential for treating various inflammatory diseases.

Keywords cyclosporine A · intraocular delivery · microneedles · polyvinylpyrrolidone

Introduction

Treatment of the back of eye disorders such as posterior uveitis, age-related macular degeneration (AMD), diabetic macular edema (DME), diabetic retinopathy (DR), cytomegalovirus retinitis (CMV), and retinitis pigmentosa (RP) is currently accomplished by invasive methods such as surgical implants and ocular injections into the vitreous humor. The invasive methods have many disadvantages such as fear of surgery, pain due to injection, and the risk of infection. Topical ophthalmic formulations such as eye drops, suspensions, and ointments have a limited ability to deliver required drug

✉ Nageeb Hassan
n.hassan@ajman.ac.ae

✉ R. Jayachandra Babu
ramapjb@auburn.edu

1 Department of Drug Discovery and Development, Auburn University, Auburn, Alabama, USA

2 Pharmaceutics and Pharmaceutical Technology Department, College of Pharmacy, Taibah University, Medina, Saudi Arabia

3 Department of Biosystems Engineering, Samuel Ginn College of Engineering, Auburn University, Auburn, Alabama 36849, USA

4 Department of Pharmaceutical Sciences, Texas A&M University, Kingsville, Texas, USA

5 Department of Pharmaceutical Sciences, College of Pharmacy and Health Sciences, Ajman University, Ajman, United Arab Emirates

6 Center of Medical and Bio-Allied Health Sciences Research, Ajman University, P.O. Box 346, Ajman, United Arab Emirates

7 Department of Clinical Sciences, College of Pharmacy and Health Sciences, Ajman University, Ajman, United Arab Emirates

8 Department of Pharmaceutical Sciences, College of Pharmacy, University of Arkansas of Medical Sciences, Little Rock, Arkansas, USA

9 Department of Pathobiology, College of Veterinary Medicine, Auburn University, 240B Greene Hall, Auburn, Alabama 36849, USA

concentrations to the back of the eye due to the protective mechanisms of the eye such as tear turnover, blinking of eyelids, and nasolacrimal drainage [1]. These protective mechanisms result in low retention of drugs in the pre-corneal region. In addition, the barrier properties of the cornea, blood-aqueous and blood-retinal barrier limit the movement of topically applied drugs into the posterior segment of the eye. Furthermore, drug metabolism by cytochrome p450 reductase and esterases in the vitreous and melanin binding of drugs in the iris and ciliary body might alter the drug pharmacokinetics [2]. These barriers result in typically less than 5% ocular bioavailability of conventional ophthalmic formulations [3]. Hence, microneedle (MN)-based ocular devices are being developed to overcome ocular barriers for the effective delivery of drugs in required concentrations [4–7]. The use of MNs for the posterior eye offers a better mode of drug delivery, which ensures improved outcomes in patients due to its less invasive nature.

Cyclosporine (CsA) is a cyclic undecapeptide with potent immunosuppressive activity. It impedes T cell activation by blocking the gene transcription responsible for the production of interleukin-2 and interleukin-4 [8]. CsA eye drops are generally preferred for treating ocular surface inflammatory diseases, while for intraocular inflammation such as uveitic conditions requiring long-term corticosteroid-sparing immunosuppression, systemic CsA in combination with other immunosuppressive agents is administered [9]. While topical ophthalmic application of CsA has a limited ocular bioavailability due to its high molecular weight (1202.6 Da) and low aqueous solubility (40 µg/mL) [10], systemic administration results in adverse effects such as nephrotoxicity, hypertension, and anemia [11, 12]. In addition, due to the presence of permeation barriers, lymphatic clearance, and lacrimation, the amount of CsA penetration from the topical formulations is limited [13].

Because of these limitations, novel strategies are being developed to improve ocular bioavailability of CsA. Numerous innovative delivery systems such micelles [14], liposomes [15], *in situ* gelling systems [16], and hydrogels [17] and contact-lens-embedded MNs [18] have been evaluated for delivering CsA to the eye. MNs have gained attention in the recent past due to their ability to localize drug action to the target ocular tissues, especially to the posterior segment of the eye, while being minimally invasive in nature. In addition, MNs offer less tissue trauma than injections or implants [19]. Various microneedle-based ocular delivery systems such as hollow MNs [20, 21], dissolvable MNs [22], and solid-coated MNs [23] have been explored previously. Microneedle arrays with longer needles can be fabricated to pierce the sclera and deliver a higher concentration of the drug to the posterior segment tissues. MNs can be designed from a wide variety of polymers in different shapes. The modulation of drug release can be achieved through the utilization of either slow-dissolving polymers, such as PLA and PLGA, or rapidly dissolvable polymers like povidone, carboxymethyl cellulose, hyaluronic acid, and chitosan [24]. Rapidly dissolvable MN advantages include (i) rapid drug release, (ii) effective drug delivery by microchannels temporarily formed by the MNs, and (iii) ability to deliver a relatively large portions of drug [25, 26]. The drawbacks associated with solid and hollow MNs, such as accidental retinal damage and detachment, since they dissolve within the ocular tissues can be avoided by the usage of dissolving microneedles [27]. An earlier study has shown that MN contact lens of CsA would meaningfully improve the drug permeation and retention in the corneal membrane [18]. However, no studies published in the literature examined the utility of microneedles in delivering CsA to the back of the eye disorders.

Polyvinylpyrrolidone (PVP) or povidone is a non-toxic, water soluble polymer approved by the FDA for various administration routes including ophthalmic route [28]. Dissolving MNs tend to soften and dissolve rapidly within the eye following penetration. This prevents damage to the ocular tissues due to mechanical forces of needle application [29]. Enhanced drug delivery and bioavailability to the posterior segment (retina) can be achieved compared to the topical and systemic administration by targeting the suprachoiroidal space (SCS) [30]. The research aims to develop dissolvable MNs for the rapid release of CsA to the SCS, for enhanced delivery into various posterior ocular tissue as a potential treatment of posterior eye inflammatory conditions.

Materials and Methods

Materials

Cyclosporine A (CsA) was procured from Letco Medical (Decatur, AL, USA). Polyvinyl pyrrolidone (Plasdone™ K 29–32) was obtained as a gift from Ashland Inc (Covington, KY, USA). Fluorescein isothiocyanate (FITC) was obtained from Alfa Aesar (Ward Hill, MA, USA). Room temperature vulcanizing (RTV) polydimethylsiloxane (PDMS) silicone microneedle molds were obtained from Micropoint Technologies Pvt. Ltd, Singapore. Trypan Blue was procured from Sigma-Aldrich (St. Louis, MO). All the other solvents used in the study were of analytical or HPLC grade.

Preparation of CsA-Loaded PVP Hydrogels

PVP hydrogels were prepared in deionized water as per the composition shown in Table I. PVP was accurately weighed, added to deionized water, vortexed for several minutes, sonicated for 1 h at 37°C, and placed overnight at room temperature for hydration. Later, the gels were used to fabricate

Table I Composition of PVP-Based MNs

Formulation	PVP conc		CsA content		PVP backing layer (no CsA)		
	(%, w/v)	g/0.5 mL	(%, w/w)	mg/0.5 mL	(%, w/v)	g/0.5 mL	mL/mold
F1	30	0.15	1.0	5.0	30	0.15	0.05
F2	50	0.25	1.0	5.0	50	0.25	0.05
F3	70	0.35	1.0	5.0	70	0.35	0.05

PVP, polyvinylpyrrolidone; *CsA*, cyclosporine A

CsA-containing hydrogel formulations. A stock solution (1 mg/mL) of CsA in acetonitrile (ACN) was prepared. CsA was added in a specified quantity to the PVP hydrogel to attain a final drug concentration of 0.5 mg/50 µL hydrogel. The hydrogel was uniformly mixed at 400 rpm for 5 h at room temperature. All formulations were stored in the refrigerator (4–8°C) in a sealed container until further use.

Fabrication of Rapid Dissolving PVP Microneedles

Each RTV PDMS silicone MN mold was added with 50 µL of the formulation and using a benchtop centrifuge (Beckman Coulter Allegra™ 6R), the molds were centrifuged for 30 min at 3300 rpm (Indiananapolis, IN). Following centrifugation, a backing layer was added by placing a drop of PVP (without CsA) into the MNs molds. Finally, the MN arrays were placed in a chemical fume hood at ambient temperature for drying.

High-Performance Liquid Chromatography (HPLC) Analysis

A Waters HPLC with an Alliance Waters e2695 Separations Module attached to a Waters 2998 PDA Detector was employed for CsA analysis. The system was interfaced with Empower 3 software. A Luna reversed phase C18 [2] 5 µm (150 mm × 4.60 mm) HPLC column was employed for CsA analysis. Eighty percent of acetonitrile in water containing 0.1% trifluoroacetic acid (TFA) was used as mobile phase. Samples (20 µL) were eluted at a 1 mL/min flow rate and temperature of 60°C and absorbance wavelength of 210 nm. The calibration curve was generated using six concentration points in the range of 1–200 µg/mL. The method was selective for CsA, linear, precise with good resolution and peak purity and was highly sensitive. The assay standard was prepared by adding 5 mg of CsA to the mobile phase. The working concentration of CsA standard was 100 µg/mL.

Characterization of Microneedle Patches Containing CsA

Structure and uniformity of MNs were analyzed using a SEM (Jeol 7000f Scanning Electron Microscope, Peabody, MA, USA). A gold coating of 20–22 nm was applied to each MN array prior to SEM analysis.

CsA content in MNs was determined by submerging the MN arrays in 8 mL of simulated lacrimal fluid (SLF, pH = 7.4) in a water bath (37°C) for 5 min. SLF contains 1.7 g/l of KCl, 2.1 g/l of $NaHCO_3$, 47.6 mg/l of $MgCl_2$, 44.4 mg/l of $CaCl_2$, and 6.3 g/l of NaCl and the pH was adjusted to 7.4 with 0.1N HCl [31]. Ethanol was added to ensure the sink condition of the experiment due to the poor solubility of the drug in SLF, pH = 7.4. The samples were analyzed via HPLC.

Microneedle Array Dissolution Studies

To measure the release of CsA from the MNs, an individual array was attached to the bottom of the wells in a 6-well plate. The plate was submerged in 5 mL dissolution media consisting of 70:30 SLF:ethanol at 37°C. After 1, 2, 3, 4, and 5 min, entire volume was collected and replaced with fresh media. The drug samples were quantified using the HPLC method described above.

Determination of Failure Force

Microneedle failure force was analyzed in order to determine MN strength. Stress–strain plots were obtained using a TA-HDi Texture Analyzer displacement-force test station (Texture Technologies Corp, Hamilton, MA). Each MN array was pressed against a stainless steel surface at a constant rate (1 mm/s) until a preset distance of 1 mm was reached. The force at which there was a sudden drop in the applied force was considered as MN failure force and the average of three runs was reported as mean ± SD.

Visualizing MN Penetration and Insertion Pathway

Fresh porcine eyes were procured from Lambert-Powell Meats Laboratory (Auburn University, Auburn, AL). Precautions were taken to maintain the integrity of the entire globe by using the eyes within 4 h of euthanasia. Animal sacrifice was carried out according to the IACUC approved protocol (SOP 2015–2727). MNs were pressed against the scleral section for 5 min and Trypan Blue staining was used to confirm the insertion and penetration of the MNs into the

scleral tissue. After penetration of MNs into scleral tissue, 50 µL of Trypan Blue was dispensed onto the injection site. After 60 s, excess Trypan Blue was rinsed from the sclera tissue and the sample was visualized by microscopy. In addition, MNs were visualized to observe PVP-based MN array dissolution after inserting MNs into the sclera for 1 min.

Ocular Distribution of CsA and FITC in Isolated Perfused Eyes

Fresh eyes from porcine were obtained as described earlier and used within 4 h of euthanizing the animal. The eyes were gently cleaned by removing excess adnexal tissue present on the ocular globe and kept in PBS pH 7.4 until usage [32]. The eyes were continuously perfused with DMEM-F12 under constant oxygen supply throughout the study duration. A major artery of each eye was located and split open with the help of a slit Eagle blade (3.0 mm). The artery was cannulated and secured with a Scotch® super glue gel and the eyes were later put in a strainer made up of stainless steel with the strainer placed on top of a beaker, which permits collection of DMEM medium from the veins. The oxygenated DMEM was perfused through the cannulated eyes with an Ismatec® peristaltic pump (Cole-Parmer GmbH, Wertheim, Germany) at a flow rate 0.25–0.8 mL/min, which was gradually increased to 1 mL/min [33]. The media flow exiting the vortex veins was used to determine the arterial perfusion. The MN patches were pressed into the sclera with the help of tweezers. For experiments, 50 µL of Restasis® was applied on the cornea surface. After 2 h, the formulation was gently removed by rising and dabbing with a tissue. The eyes were frozen immediately using solid CO_2 and later kept at 80°C to prevent the drug movement between tissues until dissection. Ocular tissues (cornea, lens, iris, vitreous humor, sclera, and retina) were separated. The frozen eye was placed on a cold ceramic tile during the separation of ocular tissues. Each tissue was soaked for 24 h by placing in HPLC mobile phase in individual vials, then filtered through a Nylon membrane filter (0.45 µm), and analyzed via HPLC.

To confirm CsA distribution within the ocular tissues, MNs made with FITC fluorescent probe were applied as described above. The eyes were quickly frozen and dissections were performed while frozen to avoid FITC transfer from one tissue to another. FITC fluorescence in the sclera and the retina was visualized immediately using a fluorescence microscope (EVOS fl, ZP-PKGA-0494 REV A, USA) at excitation (495 nm) and emission (519 nm) wavelengths.

Extraction Efficiency

The CsA extraction efficiency in various ocular tissues such as retina, sclera, cornea, iris, and vitreous humor was determined by placing the tissue samples in 2 mL of CsA solution (0.5 mg/mL) and frozen at − 20°C. The tissue samples were then minced and sonicated for 30 min. Finally, the samples were passed through a 0.45-µm nylon filter and analyzed via HPLC. The percent recovery of CsA was obtained from the ratio of the CsA amount in the spiked tissue to the CsA amount in the solution without a tissue.

Stability Study

MNs kept for 1 month protected from light in a desiccant container at room temperature. MNs were then characterized for structure and uniformity using SEM. In addition, CsA was analyzed by HPLC.

Statistical Analysis

Student *t*-test and one-way ANOVA were used for data analysis. The amount of CsA in various ocular tissues was normalized to a gram of the tissue. In all cases, statistical significance was defined at the standard 5% level. GraphPad Prism Version 4.0 (GraphPad Prism Software Inc., San Diego, CA, USA) was used for data analysis.

Results

Preparation and Characterization of Biodegradable Microneedles

Each MN array is an 8 × 8 array containing 64 microneedles with 800-µm length and 200-µm base height (Fig. 1A). Different amounts of PVP in the preparation of MN and the respective backings were selected (Table I) in order to yield MN of different hardnesses for scleral penetration while maintaining MN dissolution and CsA release. The MN tips were 20 µm in diameter, and the distance between needle tips was 680 µm. MN final weight was approximately 46, 32.5, and 28 mg for MN arrays made of 70, 50, and 30% PVP formulations, respectively. SEM analysis of MNs showed that the microneedles were sharp and uniform without any cracks, or broken tips (Fig. 1B and C). MNs must be strong and sharp so as to penetrate the sclera without breaking or bending to deliver CsA to SCS. The content of CsA in the MN arrays ranged from 93 to 98%. The MNs began to dissolve within 30 s, and they completely dissolved within 5 min for a 100% CsA release (Fig. 2). The failure force required to break MNs is marked by the steep reduction in applied force (Fig. 3). The *x*-axis represents the distance moved by the upper stage after coming in contact with MN tips. Then the stage is lowered until a set distance of 0.8 mm is reached. The MN strength was in the order: F3 > F2 > F1. A proportional increase was observed between the compression force applied and %PVP polymer used to

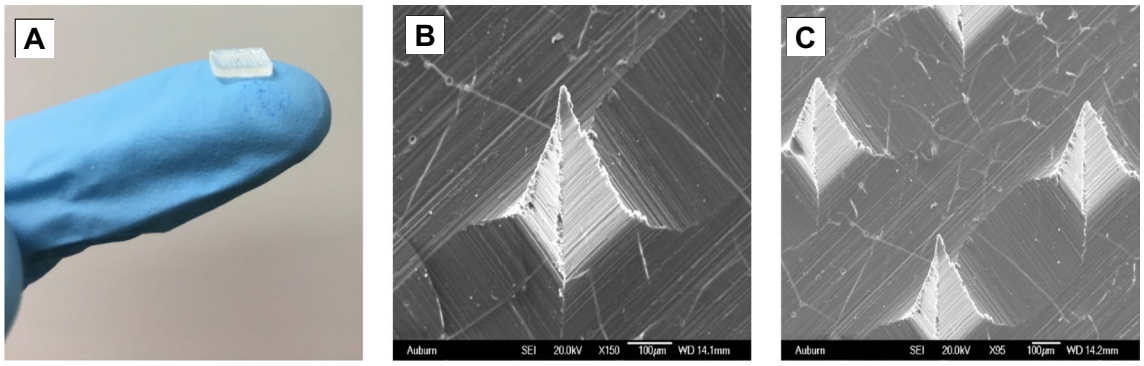

Fig. 1 PVP-based biodegradable MN arrays, 8 mm × 8 mm (**A**). The SEM image showing the structure the MN with a sharp tip, on a side view of the MN (**B**) and from the front-view of the MNs (**C**)

Fig. 2 Dissolution profiles of microneedle formulations. The values represented as mean ± standard error, $n = 3$

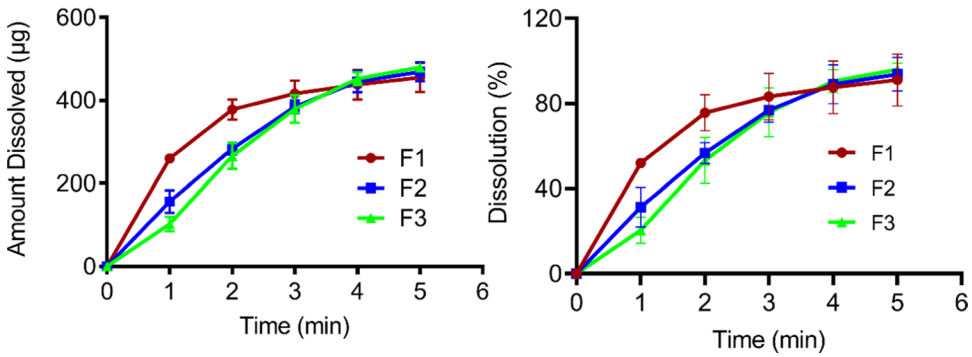

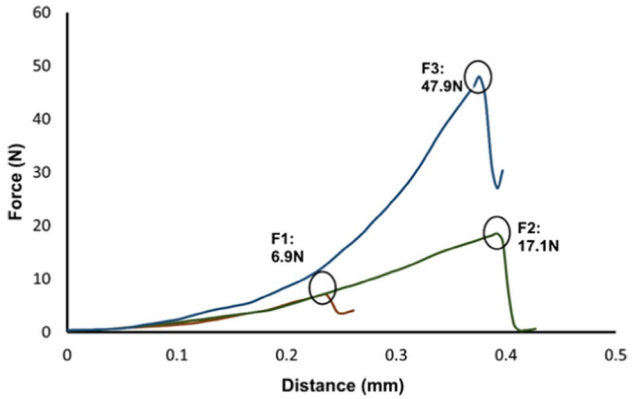

Fig. 3 Stress–strain curves from Texture Analyzer. Plot shows data until the MN failure point (dip in the curve)

fabricate the MN arrays. MNs with low PVP%, F1, broke at a shorter distance. Trypan blue was used to visualize MN-induced defects in the sclera. As shown in Fig. 4A and B, MNs were rigid enough to penetrate the sclera to deliver their drug payload into various ocular tissues. Once they penetrate the sclera, dissolving MNs will soften and rapidly dissolve (Fig. 4C), preventing ocular tissues from damage, as extended mechanical force is not required.

Ocular Distribution of CsA in Isolated Perfused Eyes

The extraction efficiency data is presented in Table II. The drug concentration obtained from various ocular tissues suggests that the recovery (extraction efficiency) was > 90% for various ocular tissues (sclera, 94.85 ± 1.356%; cornea, 94.83 ± 0.306%; retina, 95.24 ± 1.401%; iris, 99.14 ± 0.650%; lens, 98.89 ± 2.291%; VH, 92.08 ± 8.812%). Restasis® (cyclosporine 0.05% ophthalmic emulsion) eye drops are approved by the FDA for use in patients with chronic dry eye disease (DED). MNs made with 70% PVP (F3) was compared with Restasis®. CsA was observed in all ocular tissues with formulation F3. However, Restasis® had no detectable drug levels in the retina, sclera, and VH (Fig. 5). To confirm the distribution of drug within ocular tissues from MNs, FITC was traced within the ocular tissues. As shown in Fig. 6, MNs penetrated the porcine sclera and delivered FITC to both the retina and sclera.

Stability Study

The stability of MNs was studied over 1 month. The content of CsA in the MN arrays was 95 ± 5%. Even though mechanical properties have not been evaluated, SEM analysis clearly revealed that the arrays maintained their uniform shape and sharp appearance (Fig. 7) with

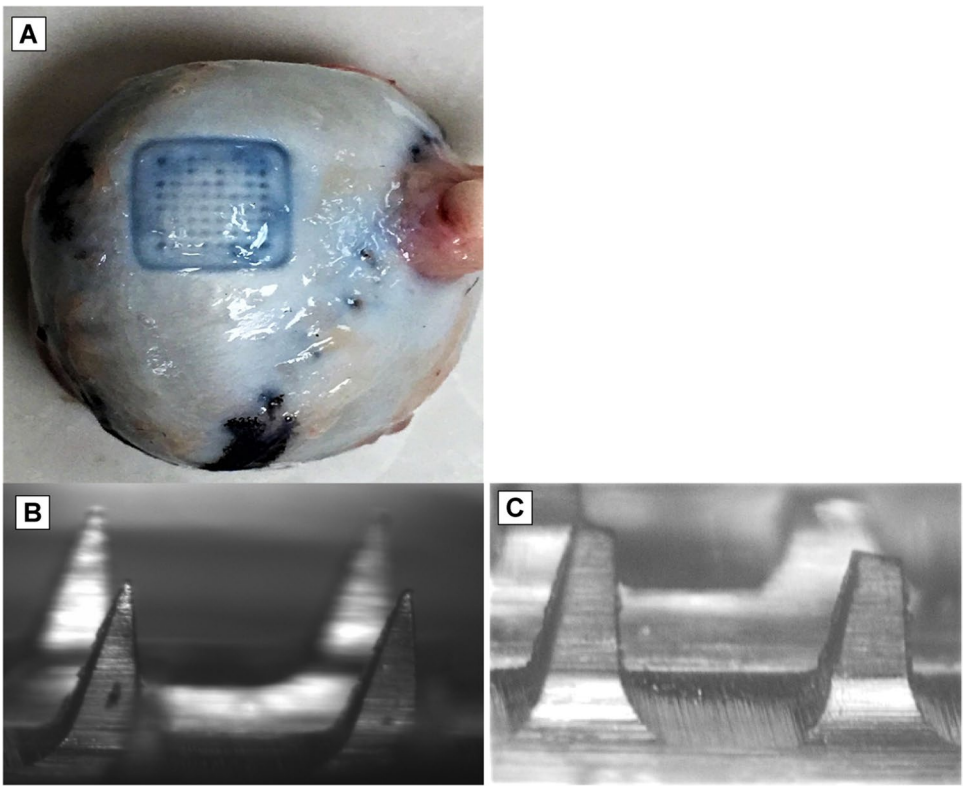

Fig. 4 **A** MN insertion points in the sclera after application showing the entire array penetrates the eyeball without failure; **B** SEM image of PVP MN arrays (F3) before insertion; and **C** after insertion into porcine scleral tissue for 60 s showing tip dissolution

Table II Validation of Ocular Drug Distribution Study: Extraction Recovery of Various Ocular Tissues Spiked with CsA

Extraction sample	Sclera	Cornea	Retina	Iris	Lens	VH
AUC-1	2,336,572	2,513,522	2,772,713	2,630,758	2,401,917	1,592,368
AUC-2	2,273,741	2,501,406	2,783,779	2,612,110	2,450,871	1,374,173
AUC-3	2,306,306	2,499,126	2,711,466	2,598,000	2,344,831	1,624,214
Recovery (µg)-1	480.95	475.88	479.23	499.07	495.05	480.51
Recovery (µg)-2	467.39	473.48	481.22	495.38	505.62	409.87
Recovery (µg)-3	474.42	473.03	468.21	492.59	482.73	490.82
% recovery-1	96.19	95.18	95.85	99.81	99.01	96.10
% recovery-2	93.48	94.70	96.24	99.08	101.12	81.97
% recovery-3	94.88	94.61	93.64	98.52	96.55	98.16
% recovery ± SD	94.85 ± 1.356	94.83 ± 0.306	95.24 ± 1.401	99.14 ± 0.650	98.89 ± 2.291	92.08 ± 8.812

VH, vitreous humor; *AUC*, area under curve

no cracks or fractures for at least 1 month. In addition, SEM analysis after 1 month showed that MN arrays had adequate stability as they maintained their shape with sharp MN tips. The stability study showed that the PVP polymer used in the fabrication of MNs had good compatibility with CsA, as there was no significant change in the content of CsA in the MN arrays after 1 month compared to the initial CsA content ($P > 0.05$).

Discussion

Diseases affecting the posterior eye, such as posterior uveitis, DR, AMD, and retinitis, are primary causes of vision loss, requiring the need for repeated administration of drugs. CsA has been widely used for treating various diseases in effecting the anterior and posterior segment of the eye. CsA, due to its high hydrophobicity (log

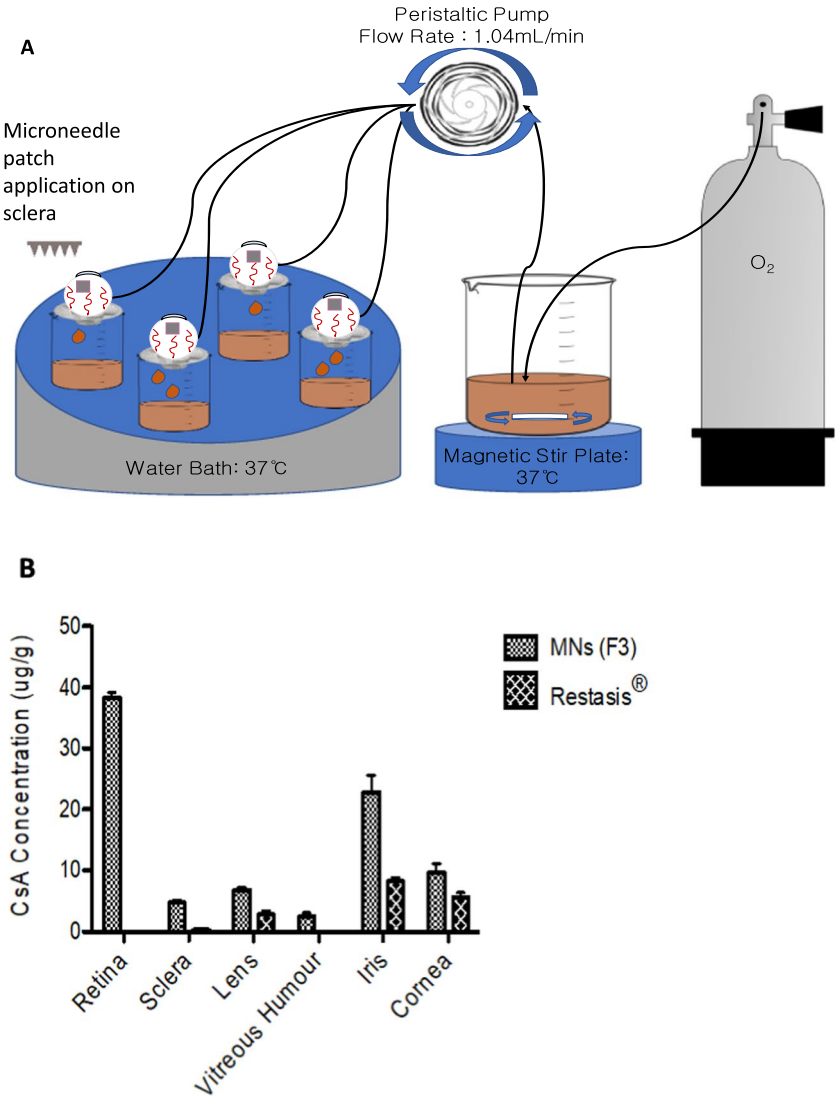

Fig. 5 **A** Perfusion eye experimental setup for ocular absorption and tissue distribution of CsA from rapidly dissolvable microneedles applied on to scleral surface. Modified from Shelley *et al*. and used with copyright permission [52]. **B** Ocular distribution of CsA in isolated porcine eyes in a continuous perfusion model after 2 h. Values represented as mean ± SD, $n = 3$

$P = 4.12$), low aqueous solubility (7.3 µg/mL) [34–37], and high molecular weight (1202 Da), topical penetration of CsA is very poor. Similarly, oral administration of CsA causes serious systemic toxicity such as nephrotoxicity and hypertension [38–40]. Therefore, there is a need to develop novel formulations that can improve ocular bioavailability and reduce adverse effects associated with currently marketed formulations.

Other delivery routes such as periocular or intravitreal administration are invasive in nature with poor patient compliance. Moreover, after injecting the drug, it is not possible to stop the drug action if toxic effects such as retinal inflammation are observed. MNs have gained popularity in ophthalmic drug delivery due to their ability to minimize tissue damage, prevent the risk of pathogen-related infections, provide faster healing, and improve the overall patient safety. MNs enable precise targeting to the SCS, thereby increasing the drug concentrations in between the sclera and the choroid. In addition, due to the unique anatomy of the eye, MNs does not infuse the drug in all directions as observed with conventional injections, rather it infuses the drug circumferentially within the SCS thereby covering a significant portion of the posterior eye even with a single administration [5].

This research shows that utilizing MNs to target SCS may be a viable option due to its ease of administration, safety, and enhanced targeting ability. Thus, MNs help in achieving higher drug levels and dosage accuracy with reduced exposure to non-target tissues compared to the marketed formulation [41–43]. Microneedles made of polymers are advantageous over metal or silicone-based needles due to its increased drug loading, rapid dissolution, and biocompatibility [44].

PVP-based MNs are rapidly dissolved after application. PVP is a biocompatible polymer which is commonly used to prepare MNs for ocular applications [22]. In this research,

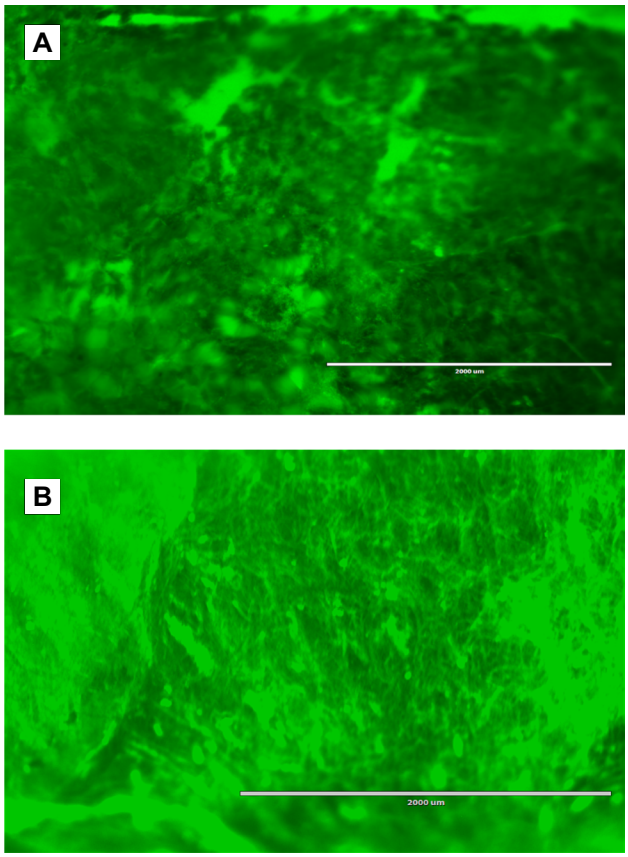

Fig. 6 Image of the retina (**A**) and the sclera (**B**) after application of MNs (F3) loaded with FITC

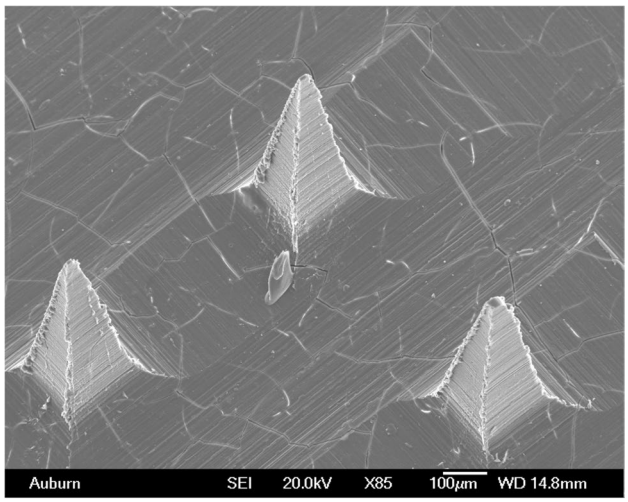

Fig. 7 SEM images revealing structure and sharpness of MNs upon 1-month storage

dissolvable MN arrays of 800-μm length were fabricated, which permit easy insertion into the sclera. This enables the drug release into the SCS, between the sclera and choroid, without penetrating the chorioretina [5]. Localized delivery to the SCS can result in higher concentration of CsA in the retina compared to topical formulations [45]. The diameter of MN tips was 20 μm, and the distance between needle tips was 680 μm. Due to its shorter and narrower needle tips, MNs causes less trauma to the eye, avoiding the need for surgical procedures and risk of infection and bleeding compared to conventional needles [46]. The final weight of the MNs were approximately 46, 32.5, and 28 mg for MN arrays made of 70, 50, and 30% PVP formulations, respectively. These polymer concentrations were sufficient enough to produce rigid MN arrays with encapsulated CsA without compromising MN dissolution rate (discussed later). The MN arrays were uniform and sharp enough to pierce the ocular tissues without bending or fracturing to deliver CsA to SCS, as shown by the SEM images (Fig. 1).

Dissolving MNs could enable the delivery of a high dose of drugs with large molecular weight because they allow the entrapment of drugs within the polymeric matrix [6]. The polymer was rapidly dissolved (30 s), leaving the drug particles in the dissolution medium, and the particles also dissolved quickly due to the presence of 30% ethanol in the dissolution medium. The dissolution time of microneedles reported in this study is slightly lower than the previously reported values by Datta *et al.* [18]. This could be due to the presence of 30% ethanol in the dissolution media, which acts as a good solvent for the dissolution of PVP. In the *in vivo* situation, the particles would remain in suspended form and would show sustained action for a prolonged time. The goal of the *in vitro* experiment was mostly to show microneedle dissolution rather than drug dissolution and quantitative expression of the MN dissolution profile. Being fabricated from a hydrophilic polymer, PVP MNs rapidly dissolved within the ocular tissues due to high water solubility [6] (Fig. 2). This rapid dissolution may increase the patient's compliance because wearing the patches for a long period of time is not necessary [47]. In addition to rapid dissolution, polymer from dissolved MNs must not bind the drug and reduce its diffusion rate since sustained release is not required. Complete CsA release from dissolved MNs indicates that the drug freely diffuses into the receptor solution.

The MN failure force study revealed the mechanical strength of the microneedles, as shown by the texture analysis data in Fig. 3. The mechanical strength and mechanical properties of dissolving MNs are dependent on affected by several factors, including polymer type and concentration, drug type, and concentration [22, 48]. In this study, higher polymer concentration helped achieve higher mechanical strength for the MN. In contrast, MNs with lower concentrations of polymer fractured at a shorter distance compared to others. Comparable results were observed in a previous study by Shelley *et al.* (2022) where the strength of the microneedles was found to be directly proportional to the

molecular weight of the polymer [7]. An essential factor in the successful development and application of dissolving MNs is their ability to penetrate into the ocular tissue without fracture or delamination of MN arrays. Trypan blue staining studies showed that the needles were intact and able to penetrate the scleral tissue. No mechanical or visual defects were noted for the MNs.

The isolated perfused porcine eye model used in the present study simulated the *in vivo* conditions such as tissue viability and circulation, thus allowing CsA determination in the individual ocular tissues. The CsA quantification method in various ocular tissues was validated to ensure that the drug was extracted well with a minimal process loss (Table II). MNs made with 70% PVP (F3) showed a similar release profile and drug content as F1 and F2. However, we selected F3 since it showed the best needle strength. Due to the presence of anterior permeation barriers such as the cornea and tear film, the amount of CsA in the posterior segment is often undetectable [49]. Dissolving MNs successfully delivered CsA in the SCS. The rapid dissolution of MNs leads to the quick release of CsA from MNs and its penetration in various ocular tissues. This strategy requires a shorter application time, which could improve patient acceptability [50]. MNs also increase CsA retention in the sclera as the drug is unperturbed by the protective properties of the eye [6]. The distribution of drug within ocular tissues after MN application was confirmed by the presence of fluorescence from FITC in the retina. No sign of hemorrhage was observed in isolated porcine eyes after the application of MN patch. It is also noteworthy to mention that the MNs fabricated in the current study are fast dissolving and does not require continued contact with the eyeball surface thereby minimizing risk of side effects such as tissue damage, irritation, inflammation, and infection [51]. In our study, we designed transcleral MN for posterior eye delivery and were able to achieve high retinal concentrations within 2 h of application of the patch in a viable perfusion eyeball model that we have previously established [52]. We allowed 2-h equilibration time before sampling each tissue because the drug that is released from the microneedle dissolution should penetrate and distribute to various ocular tissue.

The use of dissolvable MNs can be considered as a viable approach for localized delivery of drugs to the posterior eye for treating back of the eye diseases. Many drugs such as amphotericin B [53], dexamethasone [54], triamcinolone acetonide [55], and fluconazole [56] have been successfully delivered for treating the ocular inflammation or infection affecting the eye.

The amount of CsA penetration from the topical formulations is limited for the treatment of posterior eye inflammatory conditions like uveitis. Following topical application of Restasis® in New Zealand White Rabbits, negligible concentrations were observed in posterior eye tissues such as vitreous humor, choroid, and retina [57]. Hence, the dissolving MNs for CsA delivery as proposed in this research appears very promising. Even though the microneedles are safe for human use and poses a minimum risk of infection, the poked sites might act as a possible cause of infection if microneedles are not properly sterilized. Therefore, radiation sterilization, such as gamma rays and electron beam, will be utilized for terminal sterilization of biomedical devices. Previous studies have shown that microneedles fabricated with PVP K90 did not show any change in microstructure, morphology, and dissolution when exposed to gamma radiation of dose 25 kGy [58].

However, there is no sufficient data regarding the safety of microneedles for ophthalmic administration. Therefore, more studies are required to understand the long-term safety of MNs in ocular application. Finally, due to inherent simplicity and compatibility of MNs, delivery to the SCS is a straightforward approach without the need for surgical procedures commonly utilized for conventional SCS delivery [59].

Conclusion

This study demonstrated the design, fabrication, and characterization of rapidly dissolving MNs composed of PVP to overcome various ocular barriers to improve ocular drug delivery of CsA to the back of the eye. MNs dissolved rapidly (less than 5 min) within the sclera and released encapsulated CsA effectively (around 98%). MNs could resist the force needed for insertion in the eye and penetration of the sclera tissue without breaking. CsA level in posterior eye tissues was significantly higher than CsA ophthalmic emulsion (Restasis®) in the perfusion eye model. To conclude, rapidly dissolving MNs fabricated with PVP is a promising platform to deliver CsA to the posterior segment of the eye.

Abbreviations ACN: Acetonitrile; CsA: Cyclosporine A; FITC: Fluorescein isothiocyanate; HPLC: High-performance liquid chromatography; MNs: Microneedles; PDMS: Polydimethylsiloxane; PLA: Polylactic acid; PLGA: Poly (lactic-co-glycolic) acid; PVP: Polyvinylpyrrolidone; SEM: Scanning electron microscopy; SLF: Simulated lacrimal fluid; TFA: Trifluoroacetic acid

Acknowledgements The authors would like to acknowledge Lambert-Powell Meats Laboratory, Auburn University, for supplying porcine eyeballs.

Author Contribution HA: conceptualization, methodology, investigation, writing—original draft. MA: methodology, investigation, writing—original draft, writing—review and editing. OF: methodology, investigation, resources, writing—review and editing, supervision. SP: methodology, resources, writing—review and editing, supervision. SHSB: conceptualization, resources, writing—review and editing, supervision. NAGMH: resources, writing—review and editing, supervision. AKT: methodology, resources, writing—review and editing, supervision. AS: methodology, resources, writing—review and editing, supervision. RJB: conceptualization, methodology, validation, resources, writing—original draft, writing—review and editing, visualization, supervision, funding acquisition. All authors agree with their contribution.

Funding The authors acknowledge internal funds from Harrison College of Pharmacy, Auburn University. The authors thank Ajman University, College of Pharmacy and Health Sciences, for partially supporting this study through the internal research grant number 2021-IRG-PH-5.

Data Availability This manuscript has no datasets publicly available.

Declarations

Conflict of Interest The authors declare no competing interests.

References

1. Bisht R, Mandal A, Jaiswal JK, Rupenthal ID. Nanocarrier mediated retinal drug delivery: overcoming ocular barriers to treat posterior eye diseases. Wiley Interdiscip Rev Nanomed Nanobiotechnol. 2018;10(2):e1473.
2. Worakul N, Robinson JR. Ocular pharmacokinetics/pharmacodynamics. Eur J Pharm Biopharm. 1997;44(1):71–83.
3. Thrimawithana TR, Young S, Bunt CR, Green C, Alany RG. Drug delivery to the posterior segment of the eye. Drug Discovery Today. 2011;16(5–6):270–7.
4. Gote V, Sikder S, Sicotte J, Pal D. Ocular drug delivery: present innovations and future challenges. J Pharmacol Exp Ther. 2019;370(3):602–24.
5. Patel SR, Lin ASP, Edelhauser HF, Prausnitz MR. Suprachoroidal drug delivery to the back of the eye using hollow microneedles. Pharm Res. 2011;28(1):166–76.
6. Than A, Liu C, Chang H, Duong PK, Cheung CMG, Xu C, et al. Self-implantable double-layered micro-drug-reservoirs for efficient and controlled ocular drug delivery. Nat Commun. 2018;9(1):1–12.
7. Shelley H, Annaji M, Grant M, Fasina O, Babu RJ. Sustained release biodegradable microneedles of difluprednate for delivery to posterior eye. J Ocul Pharmacol Ther. 2022;38(6):449–58.
8. Matsuda S, Koyasu S. Mechanisms of action of cyclosporine. Immunopharmacology. 2000;47(2–3):119–25.
9. Dick AD, Rosenbaum JT, Al-Dhibi HA, Belfort R Jr, Brézin AP, Chee SP, et al. Guidance on noncorticosteroid systemic immunomodulatory therapy in noninfectious uveitis: Fundamentals Of Care for UveitiS (FOCUS) initiative. Ophthalmology. 2018;125(5):757–73.
10. Czogalla A. Oral cyclosporine A–the current picture of its liposomal and other delivery systems. Cell Mol Biol Lett. 2009;14(1):139–52.
11. Palestine AG, Nussenblatt RB, Chan CC. Side effects of systemic cyclosporine in patients not undergoing transplantation. Am J Med. 1984;77(4):652–6.
12. Agrahari V, Mandal A, Agrahari V, Trinh HM, Joseph M, Ray A, et al. A comprehensive insight on ocular pharmacokinetics. Drug Deliv Transl Res. 2016;6(6):735–54.
13. Lallemand F, Schmitt M, Bourges JL, Gurny R, Benita S, Garrigue JS. Cyclosporine A delivery to the eye: a comprehensive review of academic and industrial efforts. Eur J Pharm Biopharm. 2017;117:14–28.
14. Di Tommaso C, Bourges JL, Valamanesh F, Trubitsyn G, Torriglia A, Jeanny JC, et al. Novel micelle carriers for cyclosporin A topical ocular delivery: in vivo cornea penetration, ocular distribution and efficacy studies. Eur J Pharm Biopharm. 2012;81(2):257–64.
15. Karn PR, Cho W, Park HJ, Park JS, Hwang SJ. Characterization and stability studies of a novel liposomal cyclosporin A prepared using the supercritical fluid method: comparison with the modified conventional Bangham method. Int J Nanomed. 2013;8:365–77.
16. Wu Y, Yao J, Zhou J, Dahmani FZ. Enhanced and sustained topical ocular delivery of cyclosporine A in thermosensitive hyaluronic acid-based in situ forming microgels. Int J Nanomed. 2013;8:3587–601.
17. Kapoor Y, Dixon P, Sekar P, Chauhan A. Incorporation of drug particles for extended release of cyclosporine A from polyhydroxyethyl methacrylate hydrogels. Eur J Pharm Biopharm. 2017;120:73–9.
18. Datta D, Roy G, Garg P, Venuganti VVK. Ocular delivery of cyclosporine A using dissolvable microneedle contact lens. J Drug Deliv Sci Technol. 2022;70: 103211.
19. Thakur Singh RR, Tekko I, McAvoy K, McMillan H, Jones D, Donnelly RF. Minimally invasive microneedles for ocular drug delivery. Expert Opin Drug Deliv. 2017;14(4):525–37.
20. Jiang J, Moore JS, Edelhauser HF, Prausnitz MR. Intrascleral drug delivery to the eye using hollow microneedles. Pharm Res. 2009;26(2):395–403.
21. Kim YC, Edelhauser HF, Prausnitz MR. Targeted delivery of antiglaucoma drugs to the supraciliary space using microneedles. Invest Ophthalmol Vis Sci. 2014;55(11):7387–97.
22. Thakur RRS, Tekko IA, Al-Shammari F, Ali AA, McCarthy H, Donnelly RF. Rapidly dissolving polymeric microneedles for minimally invasive intraocular drug delivery. Drug Deliv Transl Res. 2016;6(6):800–15.
23. Jiang J, Gill HS, Ghate D, McCarey BE, Patel SR, Edelhauser HF, et al. Coated microneedles for drug delivery to the eye. Invest Ophthalmol Vis Sci. 2007;48(9):4038–43.
24. Cheung K, Das DB. Microneedles for drug delivery: trends and progress. Drug Deliv. 2016;23(7):2338–54.
25. Park JH, Allen MG, Prausnitz MR. Biodegradable polymer microneedles: fabrication, mechanics and transdermal drug delivery. J Control Release. 2005;104(1):51–66.
26. Wang M, Hu L, Xu C. Recent advances in the design of polymeric microneedles for transdermal drug delivery and biosensing. Lab Chip. 2017;17(8):1373–87.
27. Bhatnagar S, Saju A, Cheerla KD, Gade SK, Garg P, Venuganti VVK. Corneal delivery of besifloxacin using rapidly dissolving polymeric microneedles. Drug Deliv Transl Res. 2018;8(3):473–83.
28. Poonguzhali R, Basha SK, Kumari VS. Synthesis and characterization of chitosan-PVP-nanocellulose composites for in-vitro wound dressing application. Int J Biol Macromol. 2017;105(Pt 1):111–20.
29. Sriyanti I, Edikresnha D, Rahma A, Munir MM, Rachmawati H, Khairurrijal K. Mangosteen pericarp extract embedded in electrospun PVP nanofiber mats: physicochemical properties and release mechanism of alpha-mangostin. Int J Nanomed. 2018;13:4927–41.

30. Jung JH, Chiang B, Grossniklaus HE, Prausnitz MR. Ocular drug delivery targeted by iontophoresis in the suprachoroidal space using a microneedle. J Control Release. 2018;277:14–22.
31. Ceulemans J, Vermeire A, Adriaens E, Remon JP, Ludwig A. Evaluation of a mucoadhesive tablet for ocular use. J Control Release. 2001;77(3):333–44.
32. Abarca EM, Salmon JH, Gilger BC. Effect of choroidal perfusion on ocular tissue distribution after intravitreal or suprachoroidal injection in an arterially perfused ex vivo pig eye model. J Ocul Pharmacol Ther. 2013;29(8):715–22.
33. Mains J, Tan LE, Wilson C, Urquhart A. A pharmacokinetic study of a combination of beta adrenoreceptor antagonists - in the isolated perfused ovine eye. Eur J Pharmaceutics Biopharm. 2012;80(2):393–401.
34. Kawabata Y, Wada K, Nakatani M, Yamada S, Onoue S. Formulation design for poorly water-soluble drugs based on biopharmaceutics classification system: basic approaches and practical applications. Int J Pharm. 2011;420(1):1–10.
35. Onoue S, Sato H, Ogawa K, Kawabata Y, Mizumoto T, Yuminoki K, et al. Improved dissolution and pharmacokinetic behavior of cyclosporine A using high-energy amorphous solid dispersion approach. Int J Pharm. 2010;399(1–2):94–101.
36. Liu C, Wu J, Shi B, Zhang Y, Gao T, Pei Y. Enhancing the bioavailability of cyclosporine a using solid dispersion containing polyoxyethylene (40) stearate. Drug Dev Ind Pharm. 2006;32(1):115–23.
37. Goyal R, Macri L, Kohn J. Formulation strategy for the delivery of cyclosporine A: comparison of two polymeric nanospheres. Sci Rep. 2015;5(1):13065.
38. Mihatsch MJ, Kyo M, Morozumi K, Yamaguchi Y, Nickeleit V, Ryffel B. The side-effects of ciclosporine-A and tacrolimus. Clin Nephrol. 1998;49(6):356–63.
39. Li C, Yang CW, Ahn HJ, Kim WY, Park CW, Park JH, et al. Colchicine suppresses osteopontin expression and inflammatory cell infiltration in chronic cyclosporine nephrotoxicity. Nephron. 2002;92(2):422–30.
40. Ganesan V, Milford DV, Taylor CM, Hulton SA, Parvaresh S, Ramani P. Cyclosporin-related nephrotoxicity in children with nephrotic syndrome. Pediatric Nephrology (Berlin, Germany). 2002;17(3):225–6.
41. Özkiriş A, Erkiliç K. Complications of intravitreal injection of triamcinolone acetonide. Can J Ophthalmol. 2005;40(1):63–8.
42. Holekamp NM, Thomas MA, Pearson A. The safety profile of long-term, high-dose intraocular corticosteroid delivery. Am J Ophthalmol. 2005;139(3):421–8.
43. Razeghinejad MR, Katz LJ. Steroid-induced iatrogenic glaucoma. Ophthalmic Res. 2012;47(2):66–80.
44. Bhatnagar S, Saju A, Cheerla KD, Gade SK, Garg P, Venuganti VVK. Corneal delivery of besifloxacin using rapidly dissolving polymeric microneedles. Drug Deliv Transl Res. 2018;8(3):473–83.
45. Tyagi P, Kadam RS, Kompella UB. Comparison of suprachoroidal drug delivery with subconjunctival and intravitreal routes using noninvasive fluorophotometry. PLoS ONE. 2012;7(10): e48188.
46. Olsen TW, Feng X, Wabner K, Conston SR, Sierra DH, Folden DV, et al. Cannulation of the suprachoroidal space: a novel drug delivery methodology to the posterior segment. Am J Ophthalmol. 2006;142(5):777–87.
47. Yang S, Feng Y, Zhang L, Chen N, Yuan W, Jin T. A scalable fabrication process of polymer microneedles. Int J Nanomed. 2012;7:1415.
48. Panda A, Shettar A, Sharma PK, Repka MA, Murthy SN. Development of lysozyme loaded microneedles for dermal applications. Int J Pharm. 2021;593: 120104.
49 BenEzra D, Maftzir G, de Courten C, Timonen P. Ocular penetration of cyclosporin A. III: The human eye. Br J Ophthalmol. 1990;74(6):350–2.
50. KeeáKim H, HyeonáLee S, YongáLee B, JináKim S, YubáSung C, KeumáJang N, et al. A comparative study of dissolving hyaluronic acid microneedles with trehalose and poly (vinyl pyrrolidone) for efficient peptide drug delivery. Biomaterials science. 2018;6(10):2566–70.
51. Gadziński P, Froelich A, Wojtyłko M, Białek A, Krysztofiak J, Osmałek T. Microneedle-based ocular drug delivery systems–recent advances and challenges. Beilstein J Nanotechnol. 2022;13(1):1167–84.
52. Shelley H, Grant M, Smith FT, Abarca EM, Babu RJ. Improved ocular delivery of nepafenac by cyclodextrin complexation. AAPS PharmSciTech. 2018;19:2554–63.
53. Albadr AA, Tekko IA, Vora LK, Ali AA, Laverty G, Donnelly RF, Thakur RR. Rapidly dissolving microneedle patch of amphotericin B for intracorneal fungal infections. Drug Delivery and Translational Research. 2022:1–13.
54. Fitaihi R, Abukhamees S, Orlu M, Craig DQM. Transscleral delivery of dexamethasone-loaded microparticles using a dissolving microneedle array. Pharmaceutics. 2023;15(6):1622.
55. Roy G, Garg P, Venuganti VVK. Microneedle scleral patch for minimally invasive delivery of triamcinolone to the posterior segment of eye. Int J Pharm. 2022;612: 121305.
56. Suriyaamporn P, Opanasopit P, Rangsimawong W, Ngawhirunpat T. Optimal design of novel microemulsions-based two-layered dissolving microneedles for delivering fluconazole in treatment of fungal eye infection. Pharmaceutics. 2022;14(3):472.
57. Weiss SL, Kramer WG. Ocular distribution of cyclosporine following topical administration of OTX-101 in New Zealand white rabbits. J Ocul Pharmacol Ther. 2019;35(7):395–402.
58. Swathi HP, AnushaMatadh V, Paul Guin J, Narasimha Murthy S, Kanni P, Varshney L, et al. Effect of gamma sterilization on the properties of microneedle array transdermal patch system. Drug Dev Ind Pharm. 2020;46(4):606–20.
59. Einmahl S, Savoldelli M, D'Hermies FO, Tabatabay C, Gurny R, Behar-Cohen F. Evaluation of a novel biomaterial in the suprachoroidal space of the rabbit eye. Invest Ophthalmol Visual Sci. 2002;43(5):1533–9.